The Extended Neyman-Pearson Hypotheses Testing Framework and its Application to Spectrum Sensing in Cognitive Wireless Communication

An Jiang, Harry Leib,

Department of Electrical Engineering

McGill University

Montreal, Quebec, Canada,

Email: an.jiang@mail.mcgill.ca, harry.leib@mcgill.ca

Abstract

Neyman Person (NP) testing for two hypotheses is widely used in radar system, spectrum

sensing, medical detection and many other applications. Traditional NP testing maximizes the probability of detection under a probability of false alarm constraint. This paper consider an extended form of the NP test that is suitable for spectrum sensing when there might be different type of primary signals.

Index Terms

Neyman Pearson, Hypothesis Testing, Spectrum Sensin, Cognitive Radio

I. Introduction

The increasing radio spectrum demand for wireless communication is driving the development of new approaches for its usage, such as Cognitive Radio (CR)[1]. The concept behind CR networks is the unlicensed use of radio spectrum while ensuring no interference to the licensed users. [2]. To achieve this goal, a CR system must have "cognitive" abilities to identify opportunities for communication[3]. In CR systems, the spectrum sensing component brings in such capabilities [4].

Spectrum sensing has been a subject for extensive studies in the last years[5]. Common techniques for spectrum sensing are based on energy detection, exploitation of cyclostationarity properties of the signal being sensed, and also could use preamble sequences that are embedded in the signals [6]. In [7], the authors point out that for OFDM signals when the

variances of the noise and signal are known, the performance of energy based spectrum sensing is very close to optimal. Cooperative spectrum sensing [8], employing multiple sensors that are geographically scattered, are effective against shadowing. Different sensing algorithms and DSP techniques have been introduced for specific situations, such as in [9] where the authors study algorithms for wide band spectrum sensing focusing on sub-Neyquist sampling techniques. In [10] and [11] the authors propose compressed sensing and sub-Nyquist sampling techniques for wide band spectrum sensing.

In order to detect a free frequency channel, a spectrum sensing scheme solves a binary hypotheses testing problem, where the null hypothesis refers to the event that a user is not using the channel and the alternative hypothesis refers to the event that a user is occupying the channel. If the a-prior probabilities of null and alternative hypotheses are known, then such a problem can be solved using a Bayesian framework [12]. The situation when Baysian framework could be used is considered in [13] and the performance of such scheme is analyzed. Even though the Baysian framework can be used in some situations, in more often cases, the a-prior probabilities are not available. In such situations Neyman Pearson testing is employed [12].When there is a single type of primary user (two hypotheses), NP testing will achieve the largest probability of detecting a vacant channel when no primary user is present under a constraint on the probability that the channel will be declared vacant

when in fact a primary user is present. Traditional NP testing has been extensively used for two hypotheses problem. In such cases, the performance is characterized by the Receiver Operating Characteristic (ROC) curve, which represents the relationship between probability of detection and probability of false alarm [12].

In spectrum sensing application, there may be more than one type of primary users. For example in IEEE 802.22 [14] the channel can be occupied by Analog-TV Digital-TV and wireless microphone. In such cases, an extended NP (ENP) test can provide important advantages [15]. A detector based on ENP testing can ensure the largest probability of detection under a separate constraint of false alarm for each primary user type [16].

With an ENP detector, the achievable false alarm probabilities are limited. In this work we analyze the properties of the ENP test and propose the Modified Extended Neyman Pearson (MENP) test, that circumvents the limitations of the false alarm probabilities. The structure of the remaining of this paper is [TO BE ADDED].

II. Extended Neyman Pearson Test

A. Introduction to Extended Neyman Pearson Test

The theories of hypotheses testing have been a subject of continuous studies, and have found applications in various fields such as radar systems, spectrum sensing for cognitive communication systems, and in medical science. One type of hypotheses testing problem

can be abstracted as follows: assume $M+1$ hypotheses H_0, H_1, ..., H_M, inducing $M+1$ Probability Density Functions (PDFs) on the observable Y.

$$\begin{aligned} H_0: &\qquad Y \sim f_0(y) \\ H_1: &\qquad Y \sim f_1(y) \\ &\qquad ..... \\ H_M: &\qquad Y \sim f_M(y) \end{aligned} \tag{1}$$

Based on y, a realization of Y, the detector needs to decide whether or not it comes from $f_0(y)$. A framework for solving this problem for $M=1$ was introduced in [17] and it is commonly known as Neyman Pearson (NP) testing. The theory of NP testing was further developed in [18]. In [19], the theory of NP testing was expanded also for $M>2$. A comprehensive exposition of such generalized NP testing can be found in [16].

The Extended Neyman Pearson (ENP) Lemma: *Let $f_0(x), f_1(x), ..., f_m(x)$ be real Borel measurable functions defined on finite dimensional Euclidean space $\mathcal{R}$ such that $\int_R |f_i(x)|\mathrm{d}x < \infty (i=0,1,...,M)$. Suppose that for given constants $c_1, ..., c_M$ there exists a class of subsets $\mathcal{S}$, denoted $\mathcal{C}_\mathcal{S}$, such that for every $\mathcal{S} \in \mathcal{C}_\mathcal{S}$ we have*

$$\int_\mathcal{S} f_i(x)\mathrm{d}x = c_i, \qquad i=1,...,M \tag{2}$$

Then:

(i) *Among all members of $\mathcal{C}_{\mathcal{S}}$ there exists one that maximizes*

$$\int_{\mathcal{S}} f_0(x)\mathrm{d}x.$$

(ii) *A sufficient condition for a member of $\mathcal{C}_{\mathcal{S}}$ to maximize*

$$\int_{\mathcal{S}} f_0(x)\mathrm{d}x.$$

is the existence of constants $k_1, ..., k_M$ such that

$$f_0(x) > \sum_{j=1}^{M} k_j f_j(x) \quad \textit{when } x \in \mathcal{S} \tag{3}$$

$$f_0(x) < \sum_{j=1}^{M} k_j f_j(x) \quad \textit{when } x \notin \mathcal{S} \tag{4}$$

(iii) *If a member of $\mathcal{C}_{\mathcal{S}}$ satisfies* (3) *and* (4) *with $k_1, ..., k_M \geq 0$, then it maximizes*

$$\int_{\mathcal{S}} f_0(x)\mathrm{d}x \tag{5}$$

among all $\mathcal{S} \in \mathcal{C}_{\mathcal{S}}$ satisfying

$$\int_{\mathcal{S}} f_i(x)\mathrm{d}x \leq c_i, \quad i = 1, ..., M. \tag{6}$$

The associated probability of detection, P_d and false alarms P_{f_i} for a certain subset $\mathcal{S}$ are defined as [17], $P_d = P(H_0|H_0) = \int_{\mathcal{S}} f_0(x)\mathrm{d}x, P_{f_i} = P(H_0|H_i) = \int_{\mathcal{S}} f_i(x)\mathrm{d}x \;\; i = 1, ..., M.$ Define the step function

$$u(x) = \begin{cases} 0 & x < 0 \\ 0.5 & x = 0 \\ 1 & x > 0\,, \end{cases} \tag{7}$$

Then for a subset $\mathcal{S}$ satisfying (3) and (4) we have:

$$\begin{aligned} P_d &= \int_{-\infty}^{\infty} u(f_0(x) - \sum_{j=1}^{M} k_j f_j(x)) f_0(x)\mathrm{d}x\,, \\ P_{f_i} &= \int_{-\infty}^{\infty} u(f_0(x) - \sum_{j=1}^{M} k_j f_j(x)) f_i(x)\mathrm{d}x \;\; i = 1, 2, ..., M\,. \end{aligned} \tag{8}$$

The relationship between P_d and P_{f_i} can be represented by Receiver Operating Characteristic (ROC) surface [16].

From to (3) (4), the ENP Decision rule δ is

$$\delta : \sum_{j=1}^{M} k_j \frac{f_j(x)}{f_0(x)} \underset{\bar{H}_0}{\overset{H_0}{\gtrless}} 1 \tag{9}$$

From the **ENP Lemma**, δ achieves the largest P_d under the constraints $P_{f_i} = c_i (i = 1, 2, ..., M)$. When $M = 1$, it achieves the largest P_d under the constraint $P_f \leq c$ [16], which is the well known and commonly used form.

For applications in spectrum sensing, H_0 denotes the hypothesis that the channel is free and H_m $(m = 1, ..., M)$ corresponds to the hypothesis that the channel is occupied by the m-th primary signal. Although we have M hypotheses, we intend to determine if the channel is free or not. Hence the problem is to find a binary test of deciding H_0 versus $\bar{H}_0$ such that P_d is maximized under the constraints $P_{f_m} \leq c_m$ $m = 1, ..., M$. In context of spectrum sensing, $1 - P_{f_m}$ can be interpreted as the protection level of the $m-$th primary signal. The larger is this protection level, the smaller is the probability that when the $m-$th signal is active, the test will not detect it and will declare the channel free. In context of spectrum sensing the solution of the ENP problem maximizes the probability of detecting a free channel under a constraint on the protection level for each primary signal. The protection levels of primary signals can be different and they are guaranteed.

B. Properties of Extended Neyman Pearson Test

We consider now several properties for the ENP test, embodied by three lemmas with proof placed in the appendix.

Condition 1 *Let* $f_i(x) \quad i = 0, 1, ..., M$ *be the PDF induced by hypothesis* H_i*, and define* $g(x) = f_0(x) - \sum_{j=1}^{M} k_j f_j(x)$ *where* k_i *(*$i = 1, 2, ..., M$*) are real numbers. Let* $\mathcal{D} \in \mathbb{R}$ *be an open set such that* $\int_{\bar{\mathcal{D}}} f_i(x) = 0 \quad i = 1, 2, ..., M$*. Furthermore, if* x_0 *is a solution for* $g(x) = 0 \ \ (x \in \mathcal{D})$*, there exists an integer* n *such that the* n *order derivative of* $g(x_0)$ *is not equal to zero* $(g^{(n)}(x_0) \neq 0)$*.*

Lemma 1 *Under* **Condition 1** *, let* $\mathbf{P}$ *be a point with coordinate* $(P_d, P_{f_1}, ..., P_{f_M})$ *on the ROC surface of the EPN test. If there exists a tangent hyperplane at* $\mathbf{P}$*, then its normal is parallel to the vector* $\mathbf{n} = (-1, k_1, ..., k_M)$*, where* k_i *are the parameters of the ENP test achieving* $\mathbf{P}$*.*

Lemma 2 *Under* **Condition 1** *, let* $\mathbf{P}$ *be a point on the ROC surface,* $\left.\frac{\partial P_d}{\partial P_{f_i}}\right|_P = k_i$*, where* k_i *are the parameters of ENP test achieving* $\mathbf{P}$*.*

Lemma 3 *Under* **Condition 1** *, let* $\mathbf{P}$ *be a point on the ROC surface. If* $\mathbf{P}$ *cannot be achieved by ENP test with all positive parameters, then there exist another point* $\mathbf{P}' \ \ (P'_d, P'_{f_1}, ..., P'_{f_M})$

on the ROC surface satisfying

$$\begin{aligned} P'_d &\geq P_d \\ P'_{f_i} &\leq P_{f_i} \quad i = 1, 2, ..., M \, . \end{aligned} \tag{10}$$

C. Modified Extended Neyman Pearson Algorithm

In practice (e.g. spectrum sensing in CR communication system), the following problem needs to be solved,

$$\begin{aligned} \max \quad & P_d \\ \text{s.t.} \quad & P_{f_i} \leq c_i \quad i = 1, 2, ..., M \end{aligned} \tag{11}$$

According to ENP Lemma, this problem can by solved by ENP test only when their all parameters $k_i \geq 0, \;\; i = 1, ..., M$ such that

$$c_i = \int_{-\infty}^{\infty} u(f_0 - \sum_{j=1}^{M} k_j f_j(x)) f_i(x) \mathrm{d}x \;\; i = 1, ..., M \tag{12}$$

The case when the given $c_i \;\; i = 1, 2, ..., M$ do not satisfy (12) was not considered so far. Next we proposed the Modified Extended Neyman Pearson Test (MENP) is given considering (11).

Define $\mathbf{c}^T = [c_1, c_2, ..., c_M]$, $\mathbf{a}^T = [a_1, a_2, ..., a_M]$, $\mathbf{k}^T = [k_1, k_2, ..., k_M]$ and $\mathbf{P}_f^T = [P_{f_1}, P_{f_2}, ..., P_{f_M}]$.

Let $F(\mathbf{a})$ denote the largest P_d under the constraints $P_{f_i} = a_i \;\; i = 1, ..., M$. Also define the set $\mathcal{A}_\mathbf{c} = \{\mathbf{P}_f | 0 \leq P_{f_i} \leq c_i \;\; i = 1, 2, ..., M\}$. and set $\alpha^+ \triangleq \{\mathbf{P}_f | P_{f_i} = \int_{-\infty}^{\infty} u(f_0(x) - \sum_{j=1}^{M} k_j f_j(x)) f_i(x) \mathrm{d}x, \text{where} \;\; k_i \geq 0 \;\; i = 1, ..., M\}$.

Modified Extended Neyman Pearson test

If **Condition 1** *is satisfied, then:*

(i) *Assume* $\mathbf{c} \in \alpha^+$. *Then there must be a* $\mathbf{k}^0 = [k_1^0, k_2^0, ..., k_M^0]^T$ *with* $k_i \geq 0 \;\; i = 1, ..., M$ *satisfying*

$$P_{f_i}^0 = \int_{-\infty}^{\infty} u(f_0(x) - \sum_{j=1}^{M} k_j^0 f_j(x)) f_i(x) \mathrm{d}x = c_i \;\; (i = 1, 2, ..., M) \,. \tag{13}$$

and the decision rule δ *solving* (11) *is:*

$$\delta : \quad \frac{f_0(x)}{\sum_{i=1}^{M} k_i^0 f_i(x)} \underset{H_0}{\overset{H_0}{\gtrless}} 1 \tag{14}$$

(ii) *Assuming* $\mathbf{c} \notin \alpha^+$, *Let* $\mathcal{C} = \mathcal{A}_\mathbf{c} \cap \alpha^+$, *and* $\mathbf{a}^0 = [a_1^0, a_2^0, ..., a_M^0]^T \in \mathcal{C}$ *be such that*

$$\max_{\mathbf{a} \in \mathcal{C}} \quad F(\mathbf{a}) = F(\mathbf{a}^0) \tag{15}$$

Since $\mathbf{a}^0 \in \mathcal{A}_\mathbf{c} \cap \alpha^+$, *from* (i) *we have that there exists a different vector* $\mathbf{k}^0$ *such that* (14) *maximizes* P_d *under the constraints* $P_{f_i} = a_i^0, \;\; i = 1, ..., M$. *Here since* $a_i^0 \leq c_i^0, \;\; i = 1, ..., M$ *this decision rule satisfies* (11).

In (ii), even though the task of finding $\mathbf{a}^0$ seems to be complicated, in practice, it is not so. Since when $\mathbf{a} \in \alpha^+$ we have

$$\begin{aligned} \max \quad & P_d = F(\mathbf{a}) \\ \text{s.t.} \quad & P_{f_i} = a_i \quad i = 1, ..., M \,, \end{aligned} \tag{16}$$

when $\mathbf{a} \in \alpha^+$, according to ENP Lemma, $F(\mathbf{a})$ also satisfies

$$\begin{aligned} \max \quad & P_d = F(\mathbf{a}) \\ \text{s.t.} \quad & P_{f_i} \leq a_i \quad i = 1, ..., M \,. \end{aligned} \tag{17}$$

In (17), when one of $a_i, i = 1, ..., M$ increases and other a_i remain the same, the constraints is more relaxed, so P_d will not decrease. Hence we can conclude $F(\mathbf{a})$ is a non-decreasing function when $\mathbf{a} \in \alpha^+$. Hence we can conclude $\mathbf{a}^0$ has the largest components a_i^0 among all $\mathbf{a} \in \mathcal{C}$.

When trying to find $\mathbf{a}^0$, we only need to iterate $\mathbf{a} \in \alpha$ who have the largest components a_i instead of all $\mathbf{a} \in \alpha$.

From (i) and (ii), it can also be concluded that for any given $(c_1, c_2, ..., c_M)$, the decision rule has form given by (9) with $k_i \geq 0 \;\; i = 1, ..., M$.

The proof that MENP achieves the optimal decision rule is given in the appendix.

III. THE ROC SURFACE OF MENP

The ROC surface of MENP (M-ROC) depicts the relationship between P_d and $c_1, c_2, ..., c_M$. In one hand, it illustrates the largest P_d can that can be achieved under the constraints $P_{f_i} \leq c_i (i = 1, 2, ..., M)$, on the other hand, it provides the range of $\mathbf{c}$ for a given P_d. Points $(P_d, c_1, c_2, ..., c_M)$ on M-ROC surface can be divided into two types:

1. Those with $[c_1, c_2, ..., c_M] \in \alpha^+$. Define this set of points as M_0;

2. Those with $[c_1, c_2, ..., c_M] \notin \alpha^+$. Define this set of points as M_1. Obviously points in M_0 can be achieved by MENP (i) and points in M_1 can be achieved by MENP (ii). Next we consider a property of M-ROC surface.

Property 1

For a given $\alpha \in [0, 1)$, an M-ROC surface segment with points satisfying $P_d \geq \alpha$ is convex.

The proof is given in the appendix. Next we consider two examples that illustrate the properties of M-ROC surface for $M = 2$.

A. Gaussian Hypotheses

Assume three hypotheses given as:

$$\begin{aligned} H_0: &\qquad X \sim \mathcal{N}(-1,1) \\ H_1: &\qquad X \sim \mathcal{N}(0,1) \\ H_2: &\qquad X \sim \mathcal{N}(1,10)\,, \end{aligned} \tag{18}$$

where $\mathcal{N}(\mu,\sigma^2)$ denotes a Gaussian PDF with mean μ and variance σ^2. To form the M-ROC surface, we first consider points in region M_0.The decision rule in region M_0 is given by (9) with $M=2,\ \ k_1,k_2\geq 0$, the expression for P_d, P_{f_1} and P_{f_2} are given by (8) (according to **Neyman Pearson Lemma**, if $k_1,k_2\geq 0$, $P_{f_1}=c_1$ and $P_{f_2}=c_2$).

We use Matlab to illustrate region M_0. The values of k_1 and k_2 range from 0 to 100 with step 0.01. Substituting the value of k_1 and k_2 into (8), then we have the corresponding P_d P_{f_1} and P_{f_2}. The set M_0 is illustrated in Figure 1. Figure 2 presents the projection of Figure 1 on c_1,c_2 plane. In Figure 2, region N_0 is the projection of region M_0 on c_1-c_2 plane. Since M_0 is the set of points with $[c_1,c_2]\in\alpha^+$, N_0 is the region of points that belong to α^+. Define curve L_1 as the set of points that satisfy following conditions: (1) $(c_1,c_2)\in N_0$; (2) $(c_1,c_2+\epsilon)\notin N_0$, for any $\epsilon\geq 0$. Define curve L_2 as the set of points that satisfy the following conditions: (1) $(c_1,c_2)\in N_0$; (2) $(c_1+\epsilon,c_2)\notin N_0$, for any $\epsilon\to 0$. N_1 denotes

the region enclosed by line $c_1 = 0$, c_2; line c_1, $c_2 = 1$ and curve L_1. N_2 denotes the region enclosed by line $c_1 = 1$, c_2; line c_1, $c_2 = 0$ and curve L_2. The region of N_0 N_1 and N_2 are shown in Figure 2.

Conclusion 1

(1) All points belonging to region N_1 or curve L_1, if they have the same c_1, they have the same decision rule and same P_d.

(2) All points belonging to region N_2 or curve L_2, if they have the same c_2, they have the same decision rule and same P_d. The proof is given in the appendix.

Since we already know P_d for points in region N_0 and curves L_1 and L_2 belong to N_0, we can get the P_d for points for N_1 and N_2. M-ROC surface for this example is given in Figure 3 and the contour of M-ROC surface is given in Figure 4.

B. Chi-Square Hypotheses

Assume three hypotheses given as:

$$\begin{aligned} H_0 : &\qquad \frac{X}{\sigma_0^2} \sim \mathcal{X}^2(2N) \\ H_1 : &\qquad \frac{X}{\sigma_1^2} \sim \mathcal{X}^2(2N) \\ H_2 : &\qquad \frac{X}{\sigma_2^2} \sim \mathcal{X}^2(2N)\,, \end{aligned} \tag{19}$$

where $\mathcal{X}^2(2N)$ is the Chi-square distribution with $2N$ degree freedom(N is an integer, $\sigma_0^2 < \sigma_1^2, \sigma_2^2$ and $\sigma_1^2 \neq \sigma_2^2$). By random variable transformation[20], we can get the PDFs for different hypotheses:

$$\begin{aligned} H_0: \qquad & f_0(x) = \frac{1}{\sigma_0^2 2^N \Gamma(N)} \left(\frac{x}{\sigma_0^2}\right)^{N-1} \exp\left(-\frac{x}{2\sigma_0^2}\right) \\ H_1: \qquad & f_1(x) = \frac{1}{\sigma_1^2 2^N \Gamma(N)} \left(\frac{x}{\sigma_1^2}\right)^{N-1} \exp\left(-\frac{x}{2\sigma_1^2}\right) \\ H_2: \qquad & f_2(x) = \frac{1}{\sigma_2^2 2^N \Gamma(N)} \left(\frac{x}{\sigma_2^2}\right)^{N-1} \exp\left(-\frac{x}{2\sigma_2^2}\right) \end{aligned} \tag{20}$$

.

To form the M-ROC surface, we first consider points in region M_0. The decision rule in region M_0 is given by (9) with $k_1, k_2 \geq 0$ and $M = 2$, and the expression for P_d, P_{f_1} and P_{f_2} are given by (8) with $M = 2$ (according to **Neyman Pearson Lemma**. If $k_1, k_2 \geq 0$, $P_{f_1} = c_1$ and $P_{f_2} = c_2$).

In the following, we will prove that in this example the region achieved by ENP test with $k_1 \geq 0$ and $k_2 \geq 0$ degenerates a curve.

The decision rule for ENP test with $k_1, k_2 \geq 0$ can be written as:

$$\frac{k_1 f_1(x) + k_2 f_2(x)}{f_0(x)} \underset{H_0}{\overset{\bar{H}_0}{\gtrless}} 1 \tag{21}$$

Substituting $f_0(x), f_1(x)$ and $f_2(x)$ from (20) into (21), we get:

$$k_1' \exp\left(\frac{1}{2\sigma_0^2} - \frac{1}{2\sigma_1^2}\right)x + k_2' \exp\left(\frac{1}{2\sigma_0^2} - \frac{1}{2\sigma_2^2}\right)x \underset{H_0}{\overset{\bar{H}_0}{\gtrless}} 1 \tag{22}$$

where $k_1' = k_1(\frac{\sigma_0}{\sigma_1})^{2N}$ and $k_2' = k_2(\frac{\sigma_0}{\sigma_2})^{2N}$. Define $p_1 = \frac{1}{2\sigma_0^2} - \frac{1}{2\sigma_1^2}$ and $p_2 = \frac{1}{2\sigma_0^2} - \frac{1}{2\sigma_2^2}$, and $g(x) = k_1' \exp p_1 x + k_2' \exp p_2 x$.

The parameters k_1', k_2' are always non-negative when k_1, k_2 are such, and from the condition $\sigma_0^2 \leq \sigma_1^2$ and $\sigma_0^2 \leq \sigma_2^2$, we can conclude p_1, p_2 are positive. Hence $g(x)$ is a monotonically increasing function with x and g^{-1} exists. Assume $x_0 = g^{-1}(1)$, then the decision rule is

$$x \underset{H_0}{\overset{\bar{H}_0}{\gtrless}} x_0 \quad (x_0 \geq 0)\,. \tag{23}$$

Under decision rule (23), the expression of P_d, P_{f_1} and P_{f_2} can be written as

$$\begin{aligned} P_d &= \text{Pr}(X \leq x_0 | H_0) = F_0(x_0) \\ P_{f_1} &= \text{Pr}(X \leq x_0 | H_1) = F_1(x_0) \\ P_{f_2} &= \text{Pr}(X \leq x_0 | H_2) = F_2(x_0) \end{aligned} \tag{24}$$

where F_0, F_1 and F_2 are the CDFs of X under H_0, H_1 and H_2 that in this case are monotonically increasing functions. From (24), P_{f_1} determines x_0 that in turn determines P_{f_2}. Hence for a given P_{f_1}, there is only one corresponding P_{f_2}. Hence the ENP ROC with $k_1, k_2 \geq 0$ is a curve in this case.

By using **Conclusion 1**, we can derive the P_d for $(c_1, c_2) \notin \alpha^+$. The M-ROC surface is plotted in Figure 5 for the situation when $\sigma_0^2 = 1$, $\sigma_1^2 = 1.1$ $\sigma_2^2 = 1.15$ and $N = 120$.

IV. Energy Based Spectrum Sensing for two Primary Users

In this section, we consider an example for applying the MENP test to energy based spectrum sensing for two primary users.

A. System Model

Consider a cognitive radio system where the frequency can be occupied by one of the two distinct primary signals $\{s_1, s_2\}$ or it could be vacant. Let H_0 denote the hypothesis that the channel is vacant, and $H_i, i = 1, 2$, denote the hypothesis that the channel is occupied by primary user signal $s_i, i = 1, 2$. We test H_0 against $\overline{H}_0$ using the ENP framewor. The problem can be abstracted into following optimization problem:

$$\begin{aligned} \max \quad & P_d\,, \\ \text{s.t.} \quad & P_{f_i} \leq c_i \quad (i = 1, 2)\,. \end{aligned} \tag{25}$$

Our object is to plot the maximum P_d vs. c_1, c_2 (M-ROC).

A block diagram of system is illustrated in Figure 6. The system consists of a measuring device followed by a testing device. The role of the measuring device is to output a suitable test statistics. The role of the testing device is to decide whether the channel is free based on the output of the measuring device. The input of the measuring device is

$$x[n] = \begin{cases} \omega[n] & \text{when no primary user is occupying the channel} \\ \omega[n] + s_i[n] & \text{when primary user } i \text{ is occupying the channel}\,. \end{cases} \tag{26}$$

For $n = 1, 2, ..., N$, and $i = 1, 2$. We also assume that $s_i[n]$ and $\omega[n]$ are i.i.d. circular symmetric complex Gaussian(CSCG) random variables with variance $2\sigma_{s_i}^2$ and $2\sigma_\omega^2$, in other words, $s[n] \sim \mathcal{CN}(0, 2\sigma_{s_i}^2)$ and $\omega[n] \sim \mathcal{CN}(0, 2\sigma_\omega^2)$. Since the noise and the signal are independent, $s_i[n] + \omega[n] \sim \mathcal{CN}(0, 2(\sigma_\omega^2 + \sigma_{s_i}^2))$.

When the testing device is a energy detector, its output is

$$X = \sum_{n=1}^{N} |x[n]|^2 = \sum_{n=1}^{N} (x_R[n]^2 + x_I[n]^2)\,, \tag{27}$$

x_R and x_I are respectively the real and imaginary part of signal x. Substituting (26) into (27) and defining $\sigma_i^2 = \sigma_\omega^2 + \sigma_{s_i}^2$ we have

$$\begin{aligned} \mathcal{H}_0 : \quad & \frac{X}{\sigma_\omega^2} \sim \mathcal{X}_{2N} \\ \mathcal{H}_1 : \quad & \frac{X}{\sigma_1^2} \sim \mathcal{X}_{2N} \\ \mathcal{H}_2 : \quad & \frac{X}{\sigma_2^2} \sim \mathcal{X}_{2N} \end{aligned} \tag{28}$$

Since $\sigma_\omega^2 < \sigma_1^2, \sigma_2^2$, this problem has the same form as that of Chi-Square example given in last section. Using the conclusions given in Chi-Square example, the decision rule is

$$\delta : \quad x \underset{H_0}{\overset{H_0}{\lessgtr}} x_0 \,, \tag{29}$$

where $x_0 \in [0, \infty)$ and the corresponding P_d is given in (24). By using this decision rule, MS-ROC can be formed.

B. Simulation result

In this section, we provide both the performance analysis and the simulation result to show the performance of MENP test for energy based spectrum sensing by plotting M-ROC. Assume $\sigma_\omega^2 = 1$, $\sigma_{s_1}^2 = 0.1$, $\sigma_{s_2}^2 = 0.15$ and N=120.

In our Monte Carlo simulation, we get the corresponding P_d, c_1 and c_2 by increasing the value of λ from 0 to 100. All simulations are run until at least 400 detections (and miss detections) are observed. The outcome is plotted in Fig 8 by bold curve. After that, we

utilize **Conclusion 1** given in "Gaussian Example" to achieve the whole M-ROC surface. The whole M-ROC surface is given in Fig. 8.

V. Conclusions

In this paper, we explore the new field of spectrum sensing with emphasis on providing different levels of protections for various primary users. The proposed MENP test could achieve the largest probability of detection detection under multiple constraints of probability of false alarms. After that, we approach M-ROC surface to represent the relationship between the probability of detection and the constraint conditions. Two examples respectively concerning Gaussian distribution and Chi-Square distribution are given to show the properties of M-ROC surface. We also proposed an energy based detector for two different types of primary users. For simplicity, we assume the signal samples of the primary users subject to iid CSCG distribution and the variance of the signal and the noise are known to the detector. By simulation, we showed the performance of this detector. In this work we assume the detector has the information of the signals' variance. There are other ways dealing with unknown parameters, for example using cyclostationary property to estimate the variance of the primary users. This could be a future topic.

APPENDIX

A. Proof for Lemma 1

Define $\mathbf{k} = [k_1, k_2, ..., k_M]^T$ and $\mathbf{P}_f = [P_{f_1}, P_{f_2}, ..., P_{f_M}]^T$. Since both P_d and $\mathbf{P}_f$ are functions of $\mathbf{k}$, $\mathbf{P}_f(\mathbf{k}_0)$ denotes the value of $\mathbf{P}_f$ when $\mathbf{k} = \mathbf{k}_0$ and $P_d(\mathbf{k}_0)$ denotes the value of P_d when $\mathbf{k} = \mathbf{k}_0$. Using Taylor's expansion for $\mathbf{P}_f$ and P_d,

$$P_d = P_d(\mathbf{k}_0) + \frac{\mathrm{d}P_d}{\mathrm{d}\mathbf{k}^T}\bigg|_{\mathbf{k}=\mathbf{k_0}} (\mathbf{k} - \mathbf{k}_0) + o(\mathbf{k} - \mathbf{k}_0) \tag{30}$$

$$\mathbf{P}_f = \mathbf{P}_f(\mathbf{k}_0) + \frac{\mathrm{d}\mathbf{P}_f}{\mathrm{d}\mathbf{k}^T}\bigg|_{\mathbf{k}=\mathbf{k_0}} (\mathbf{k} - \mathbf{k}_0) + o(\mathbf{k} - \mathbf{k}_0) \tag{31}$$

here $\mathbf{k} \to \mathbf{k}_0$.

Consider the hyperplane y as a function of $\mathbf{x}$ defined by

$$\mathbf{x} = \mathbf{P}_f(\mathbf{k}_0) + \frac{\mathrm{d}\mathbf{P}_f}{\mathrm{d}\mathbf{k}^T}\bigg|_{\mathbf{k}=\mathbf{k_0}} (\mathbf{z} - \mathbf{k}_0) \tag{32}$$

$$y = P_d(\mathbf{k}_0) + \frac{\mathrm{d}P_d}{\mathrm{d}\mathbf{k}^T}\bigg|_{\mathbf{k}=\mathbf{k_0}} (\mathbf{z} - \mathbf{k}_0) \tag{33}$$

The above equations construct a tangent hyperplane for the ROC surface at point $(P_d(\mathbf{k}_0), \mathbf{P}_f^T(\mathbf{k}_0))$. Combining both equations we get

$$y = P_d(\mathbf{k}_0) + \left.\frac{\mathrm{d}P_d}{\mathrm{d}\mathbf{k}^T}\right|_{\mathbf{k}=\mathbf{k_0}} (\left.\frac{\mathrm{d}\mathbf{P}_f}{\mathrm{d}\mathbf{k}^T}\right|_{\mathbf{k}=\mathbf{k_0}})^{-1}(\mathbf{x} - \mathbf{P}_f(\mathbf{k}_0)) \tag{34}$$

Hence the normal for point $(P_d(\mathbf{k}_0), \mathbf{P}_f^T(\mathbf{k}_0))$ on ROC surface can be written as

$$[-1, \left.\frac{\mathrm{d}P_d}{\mathrm{d}\mathbf{k}^T}\right|_{\mathbf{k}=\mathbf{k_0}} (\left.\frac{\mathrm{d}\mathbf{P}_f}{\mathrm{d}\mathbf{k}^T}\right|_{\mathbf{k}=\mathbf{k_0}})^{-1}]. \tag{35}$$

In the following, we will prove $\frac{\mathrm{d}P_d}{\mathrm{d}\mathbf{k}^T}(\frac{\mathrm{d}\mathbf{P}_f}{\mathrm{d}\mathbf{k}^T})^{-1} = \mathbf{k}^T$, which can be written as

$$\frac{\mathrm{d}P_d}{\mathrm{d}\mathbf{k}^T} = \mathbf{k}^T \frac{\mathrm{d}\mathbf{P}_f}{\mathrm{d}\mathbf{k}^T} \tag{36}$$

Previous equation can be written in component form as

$$\frac{\partial P_d}{\partial k_i} - \sum_{n=1}^{M} k_n \frac{\partial P_{f_n}}{\partial k_i} = 0 \quad (i = 1, 2, ..., M). \tag{37}$$

Calculating the partial derivatives results in

$$\frac{\partial P_{f_n}}{\partial k_i} = -\int_{\mathcal{D}} \delta(f_0(x) - \sum_{j=1}^{M} k_j f_j(x)) f_i(x) f_n(x) \mathrm{d}x\,, \tag{38}$$

$$\frac{\partial P_d}{\partial k_i} = -\int_{\mathcal{D}} \delta(f_0(x) - \sum_{j=1}^{M} k_j f_j(x)) f_i(x) f_0(x) \mathrm{d}x\,, \tag{39}$$

where $\delta(\bullet)$ is Dirac's delta function defined as following,

$$\delta(x) = \lim_{\epsilon \to 0} \begin{cases} \frac{1}{\epsilon} & \text{when } \ x \in (-\frac{\epsilon}{2}, \frac{\epsilon}{2}) \\ 0 & \text{otherwise} \end{cases} \tag{40}$$

Defining $g(x) = f_0(x) - \sum_{j=1}^{M} k_j f_j(x)$, (37) can be written as $\int_{\mathcal{D}} \delta(g(x)) g(x) f_n(x) \mathrm{d}x = 0, n = 0, 1, ..., M$.

When $g(x) \neq 0$, we have $\delta(g(x)) = 0$ and $\delta(g(x))g(x)f_i(x) = 0$. When $g(x) = 0$, we can solve the equation according to the definition of $\delta(\bullet)$ and consider

$$\int_{\{x|g(x)\in(-\frac{\epsilon}{2},\frac{\epsilon}{2})\}} \frac{1}{\epsilon} g(x) f_n(x) \mathrm{d}x \quad n = 0, 1, ..., M \tag{41}$$

Since when $g(x) \in (-\frac{\epsilon}{2}, \frac{\epsilon}{2})$, $|g(x)| < \frac{\epsilon}{2}$,

$$\left| \int_{\{x|g(x)\in(-\frac{\epsilon}{2},\frac{\epsilon}{2})\}} \frac{1}{\epsilon} g(x) f_i(x) \mathrm{d}x \right| < \int_{\{x|g(x)\in(-\frac{\epsilon}{2},\frac{\epsilon}{2})\}} \frac{1}{2} f_i(x) \mathrm{d}x \tag{42}$$

Assume x_s is one of the zero point of $g(x)$, also assume $g'(x_s)$, $g^{(2)}(x_s)$, ..., $g^{(n-1)}(x_s)$ are zero but $g^{(n)}(x_s) \neq 0$ (here $n = 1, 2, ...$). Use Taylor expansion near point x_s,

$$g(x) = \frac{g^{(n)}(x_s)}{n!}(x - x_s)^n + o((x - x_s)^n)\,. \tag{43}$$

From equation (43), it can be seen when $g(x) \in (-\frac{\epsilon}{2}, \frac{\epsilon}{2})$, $x \in \left(x_s - \left(\frac{n!\varepsilon}{2|g^{(n)}(x_s)|}\right)^{\frac{1}{n}}, x_s + \left(\frac{n!\varepsilon}{2|g^{(n)}(x_s)|}\right)^{\frac{1}{n}} \right)$.

Define $\triangle x = \left(\frac{n!\varepsilon}{2|g^{(n)}(x_s)|}\right)^{\frac{1}{n}}$, when $\epsilon \to 0$, $\triangle x \to 0$ and

$$g(x) \in (-\frac{\epsilon}{2}, \frac{\epsilon}{2}) \Leftrightarrow x \in (x_s - \triangle x, x_s + \triangle x) \tag{44}$$

Hence when $\epsilon \to 0$ we have

$$\int_{\{x|g(x)\in(-\frac{\epsilon}{2},\frac{\epsilon}{2})\}} \frac{1}{2} f_i(x) \mathrm{d}x \to f_i(x_s) \triangle x \to 0 \tag{45}$$

Using the above two conclusions for $g(x) = 0$ and $g(x) \neq 0$, we get

$$\int_{\mathcal{D}} \delta(g(x)) g(x) f_i(x) \mathrm{d}x = 0 \tag{46}$$

In this way, we prove the normal for the point **P** on the ROC is $(-1, k_1, k_2, ..., k_M)$.

B. Proof for Lemma 2

The expression of tangent hyper surface for point $(P_d^0, P_{f_1}^0, ..., P_{f_M}^0)$ on the ROC hyper surface can be written as

$$P_d = P_d^0 + \sum_{i=1}^{M} \left. \frac{\partial P_d}{\partial P_{f_i}} \right|_{P_{f_i}=P_{f_i}^0} (P_{f_i} - P_{f_i}^0) \,. \tag{47}$$

Hence the normal at this point is

$\mathbf{n} = [-1, \frac{\partial P_d}{\partial P_{f_1}}, \frac{\partial P_d}{\partial P_{f_2}}, ..., \frac{\partial P_d}{\partial P_{f_M}}]$. Since we have proved that the normal for this point is $\mathbf{n} = [-1, k_1, k_2, ..., k_M]$, we must have

$$\left.\frac{\partial P_d}{\partial P_{f_i}}\right|_P = k_i \tag{48}$$

C. Proof for Lemma 3

Assume $\mathbf{P}(P_d, P_{f_1}, ..., P_{f_M})$ is a point on the ROC and it cannot be achieved by ENP test with non-negative parameters. Assume it can be achieved by ENP test with parameter $\mathbf{k} = [k_1, k_2, ..., k_M]^T$ and k_l is negative.

If there exists a tangent hyper plane at point $\mathbf{P}$, according to **Lemma 2**, $\frac{\partial P_d}{\partial P_{f_l}} = k_l < 0$. Consider another point $\mathbf{P}'(P'_d, P'_{f_1}, ..., P'_{f_M})$, here $P_{f_i} = P'_{f_i} (i \neq l)$ and $P'_{f_l} = P_{f_l} - \epsilon \ \ (\epsilon \rightarrow 0 \text{and} \epsilon > 0)$. The partial derivative can be written in following form:

$$\left.\frac{\partial P_d}{\partial P_{f_l}}\right|_{\mathbf{P}} = \frac{P_d - P'_d}{P_{f_l} - P'_{f_l}} = k_l \,. \tag{49}$$

Hence

$$P_d - P'_d = \epsilon k_l \tag{50}$$

The expression of P'_d can be written as

$$P'_d = P_d - \epsilon k_l \,. \tag{51}$$

Since $k_l < 0$, $P'_d > P_d$. By comparing $\mathbf{P}'$ with $\mathbf{P}$, we can conclude

$$\begin{aligned} P'_d &> P^0_d \\ P'_{f_i} &\leq P^0_{f_i} \qquad \text{for} \qquad i = 1, 2, ..., M\,. \end{aligned} \tag{52}$$

If there is no tangent hyper plane at point $\mathbf{P}$, we use another point to approximate $\mathbf{P}$. Assume $\mathbf{P}'(P'_d, P'_{f_1}, ..., P'_{f_M})$ is a point achieved by ENP parameters $\mathbf{k} = [k'_1, k'_2, ..., k'_M]^T$, where $k'_i = k_i$ $(i \neq s)$ (s could be any integer between 0 and M) and $k'_s = k_s + \delta$ ($\delta \to 0, \delta > 0$) and there exists a tangent hyper plane at point $\mathbf{P}'$. From (38) and (A), the expression inside the integration are all non-negative, hence we have $\frac{\partial P_{fn}}{\partial k_i}|_{P'} \leq 0$ and $\frac{\partial P_d}{\partial k_i}|_{P'} \leq 0$. Using Taylor expression for point P',

$$\begin{aligned} P_d &= P'_d + \sum_{i=1}^{M} \left.\frac{\partial P_d}{\partial k_i}\right|_{P'} (k_i - k'_i) + o(\sum_{i=1}^{M}(k_i - k'_i)^2) \\ &= P'_d - \delta \frac{\partial P_d}{\partial k_s} \geq P'_d\,. \end{aligned} \tag{53}$$

In the same method, we can prove $P'_{f_i} \leq P_{f_i}$.

Define $\alpha = P_d - P'_d$ and the expression of P_d and P'_d can be written as

$$P_d = \int_{\mathcal{S}} f_0(x)\mathrm{d}x \tag{54}$$

and

$$P'_d = \int_{\mathcal{S}'} f_0(x)\mathrm{d}x \tag{55}$$

where $\mathcal{S}$ is defined as

$$x \in \mathcal{S} \text{iff} f_0(x) \geq \sum_{j=1}^{M} k_j f_j(x) \tag{56}$$

$\mathcal{S}'$ is defined as

$$x \in \mathcal{S} \text{iff} f_0(x) \geq \sum_{j=1}^{M} k'_j f_j(x)\,. \tag{57}$$

Since $k'_i = k_i (i \neq s)$ and $k'_s \to k_s$, we know $\mathcal{S}' \to \mathcal{S}$ and $P'_d \to P_d$. We can conclude $\alpha \to 0$.

Since there exists a tangent hyperplane on the ROC surface at point $\mathbf{P}'$, there exists a point $\mathbf{P}''(P''_d, P''_{f_1}, ..., P''_{f_M})$, where $P''_d = P'_d - \epsilon k'_l$ and $P''_{f_i} \leq P'_{f_i}$. We let $\epsilon > \frac{\alpha}{|k'_l|}$ and $P''_d > P_d$. Hence for point $\mathbf{P}''$, we have

$$\begin{aligned} P''_d &> P_d \\ P''_{f_i} &\leq P_{f_i} \end{aligned} \tag{58}$$

D. Proof for MENP test

MENP test (i) is part of in **Neyman Pearson Lemma**. In the following, we will prove MENP test (ii). Define m dimension vector $\mathbf{b}^T = [b_1, b_2, ..., b_M]$, and set $\mathcal{B} = \{\mathbf{b} | b_i \in [0, c_i]\}$, c_i is given in (11). For $P_{f_i} = b_i (i = 1, 2, ..., M)$, denote the largest P_d can be given by NP

testing by $G(\mathbf{b})$. The problem given in (11) can be written as

$$\begin{aligned} \max \quad & G(\mathbf{b}) \\ \text{s.t.} \quad & \mathbf{b} \in \mathcal{B}\,. \end{aligned} \tag{59}$$

$\mathbf{b}$ can be classified into three types: (1) there only exists ENP decision rule with negative parameters can achieve $P_{f_i} = b_i (i = 1, ..., M)$; (2) no decision rule can achieve $P_{f_i} = b_i (i = 1, ..., M)$; (3) there exists ENP decision rule with all non-negative parameters can achieve $P_{f_i} = b_i (i = 1, ..., M)$, which means $\mathbf{b} \in \alpha^+$.

If a $\mathbf{b}$ belongs to type (1), according to **Lemma 3**, points in this region cannot satisfy (11), so it cannot be the solution for (59); if $\mathbf{b}$ belongs to type (2), there is no decision rule satisfying $P_{f_i} = b_i (i = 1, 2, ..., M)$, hence it cannot be the solution for (59). Hence we can conclude if $\mathbf{b}$ satisfy (59), $\mathbf{b} \in \alpha^+$. Problem given by (11) can be transform into

$$\begin{aligned} \max \quad & G(\mathbf{b}) \\ \text{s.t.} \quad & \mathbf{b} \in \mathcal{B} \cap \alpha^+\,. \end{aligned} \tag{60}$$

MENP test (ii) is proved.

E. Proof for Property 1

Define set $\mathcal{C}_\alpha = \{(P_d, c_1, c_2, ..., c_M) |$ there exists a decision rule δ that can satisfy $P_{f_i}(\delta) \leq c_i$ and $P_d(\delta) \geq \alpha\}$. Assume that point $A(P_{dA}, c_{1A}, c_{2A}, ..., c_{MA}) \in \mathcal{C}_\alpha$ and point $B(P_{dB}, c_{1B}, c_{2B}, ..., c_{MB}) \in$

$\mathcal{C}_\alpha$. Decision rule δ_A is one of the decision rules that can achieve point A; decision rule δ_B is one of the decision rules that can achieve point B. The probability of detection and probability of false alarm for decision rule δ_A is $(P_{dA}, P_{f_1A}, P_{f_2A}, ..., P_{f_MA})$; The probability of detection and probability of false alarm for decision rule δ_B is $(P_{dB}, P_{f_1B}, P_{f_2B}, ..., P_{f_MB})$.

Consider a random decision rule δ_C, which use δ_A with probability θ ($\theta \in (0, 1)$), and use δ_B with probability $1 - \theta$. Hence the probability of detection and probability of false alarm for for decision rule δ_C will be $(\theta P_{dA} + (1-\theta)P_{dB}, \theta P_{f_1A} + (1-\theta)P_{f_1B}, \theta P_{f_2A} + (1-\theta)P_{f_2B}, ..., \theta P_{f_MA} + (1-\theta)P_{f_MB})$.

Since $P_{f_iA} \leq c_{iA}$ and $P_{f_iB} \leq c_{iB}$, we can have $\theta P_{f_iA} + (1-\theta)P_{f_iB} \leq \theta c_{iA} + (1-\theta)c_{iB}$. In the same way, we know $P_{dC} \leq \alpha$. Hence, point $C \in \mathcal{C}$ and we can conclude that $\mathcal{C}$ is a convex set.

According to the definition of Leib-Jiang Algorithm, points on $\alpha-$MS-ROC achieve the maximum of P_d for the given $c_1, c_2, ..., c_M$. Hence points on $\alpha-$MS-ROC are boundary points of a convex set.

F. Proof for Conclusion 1

Consider points in region N_1. Since $(c_1, c_2) \notin N_0$, we use MENP (ii) to achieve P_d. As it is shown in Figure 2, A is a point in N_1 with coordinate (x, y). According to MENP (ii), $\mathcal{C}$ is the set of points lie in region enclosed by curve L_1 L_2 and line $c_1 = x$. For all points

belongs to $\mathcal{C}$, point B has the largest c_1 and c_2 value. As we proved function $F(c_1, c_2)$ is non-decreasing, point B has the largest P_d among all points belong to region $\mathcal{C}$. Hence we proved point A and point B have the same decision rule and same P_d. Since point in region N_1 with $c_1 = x$ has the same decision rule and P_d with point B, we can conclude: for points belong to region N_1 or curve L_1, if they have the same c_1 value, they have the same decision rule and same P_d.

In the same way, we can prove: For points belong to region N_2 or curve L_2, if they have the same c_2 value, they have the same decision rule and same P_d.

REFERENCES

[1] S. Haykin, "Cognitive radio: brain-empowered wireless communications," *Selected Areas in Communications, IEEE Journal on*, vol. 23, pp. 201 – 220, feb. 2005.

[2] A. Goldsmith, S. A. Jafar, I. Maric, and S. Srinivasa, "Breaking spectrum gridlock with cognitive radios: An information theoretic perspective," *Proceedings of the IEEE*, vol. 97, no. 5, pp. 894–914, 2009.

[3] M. M. Buddhikot, "Understanding dynamic spectrum access: Models, taxonomy and challenges," in *New Frontiers in Dynamic Spectrum Access Networks, 2007. DySPAN 2007. 2nd IEEE International Symposium on*, pp. 649–663, IEEE, 2007.

[4] R. Tandra, S. M. Mishra, and A. Sahai, "What is a spectrum hole and what does it take to recognize one?," *Proceedings of the IEEE*, vol. 97, no. 5, pp. 824–848, 2009.

[5] E. Axell, G. Leus, E. G. Larsson, and H. V. Poor, "Spectrum sensing for cognitive radio: State-of-the-art and recent advances," *Signal Processing Magazine, IEEE*, vol. 29, no. 3, pp. 101–116, 2012.

[6] D. Cabric, S. M. Mishra, and R. W. Brodersen, "Implementation issues in spectrum sensing for cognitive radios," in *Signals, systems and computers, 2004. Conference record of the thirty-eighth Asilomar conference on*, vol. 1, pp. 772–776, IEEE, 2004.

[7] E. Axell and E. G. Larsson, "Optimal and sub-optimal spectrum sensing of ofdm signals in known and unknown noise variance," *Selected Areas in Communications, IEEE Journal on*, vol. 29, no. 2, pp. 290–304, 2011.

[8] G. Ganesan and Y. Li, "Cooperative spectrum sensing in cognitive radio networks," in *New Frontiers in Dynamic Spectrum Access Networks, 2005. DySPAN 2005. 2005 First IEEE International Symposium on*, pp. 137–143, IEEE, 2005.

[9] Z. Tian and G. B. Giannakis, "Compressed sensing for wideband cognitive radios," in *Acoustics, Speech and Signal Processing, 2007. ICASSP 2007. IEEE International Conference on*, vol. 4, pp. IV–1357, IEEE, 2007.

[10] H. Sun, A. Nallanathan, C.-X. Wang, and Y. Chen, "Wideband spectrum sensing for cognitive radio networks: a survey," *Wireless Communications, IEEE*, vol. 20, no. 2, pp. 74–81, 2013.

[11] H. Sun, W.-Y. Chiu, J. Jiang, A. Nallanathan, and H. V. Poor, "Wideband spectrum sensing with sub-nyquist sampling in cognitive radios," *arXiv preprint arXiv:1302.1847*, 2013.

[12] H. V. Poor, *An introduction to signal detection and estimation*. Springer, 1994.

[13] Y. Zeng, Y.-C. Liang, A. T. Hoang, and R. Zhang, "A review on spectrum sensing for cognitive radio: challenges and solutions," *EURASIP Journal on Advances in Signal Processing*, vol. 2010, p. 2, 2010.

[14] S. J. Shellhammer *et al.*, "Spectrum sensing in ieee 802.22," *IAPR Wksp. Cognitive Info. Processing*, pp. 9–10, 2008.

[15] Q. Zhang, P. K. Varshney, and Y. Zhu, "Design of extended neyman-pearson hypothesis tests," in *AeroSense'99*, pp. 378–389, International Society for Optics and Photonics, 1999.

[16] E. L. Lehmann, *Testing statistical hypotheses*. Wiley, 1959.

[17] J. Neyman and E. Pearson, "On the problem of the most efficient tests of statistical hypotheses," *Philosophical Transactions of the Royal Society of London. Series A, Containing Papers of a Mathematical or Physical Character*, vol. 231, pp. 289–337, 1933.

[18] A. Wald, "Contributions to the theory of statistical estimation and testing hypotheses," *The Annals of Mathematical Statistics*, pp. 299–326, 1939.

[19] G. Dantzig and A. Wald, "On the fundamental lemma of neyman and pearson," *The Annals of Mathematical Statistics*, vol. 22, no. 1, pp. 87–93, 1951.

[20] B. L. Mark and W. Turin, *Probability, Random Processes, and Statistical Analysis*. Cambridge University Press Textbooks, 2011.

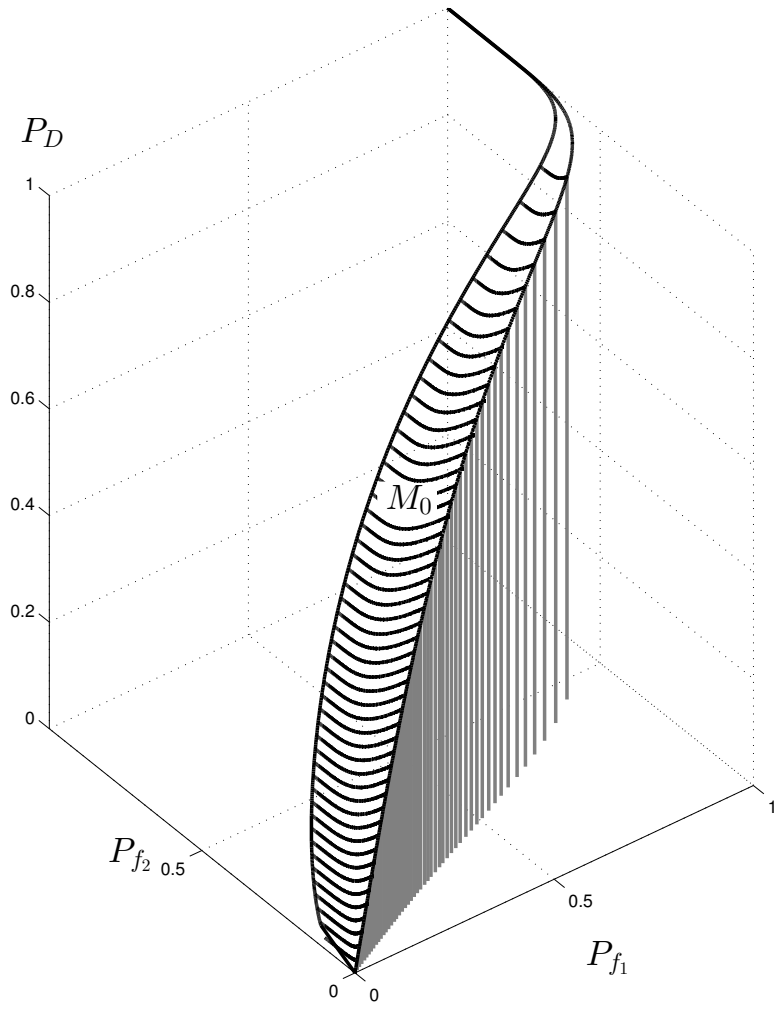

Fig. 1. Region that can be achieved by Neyman Pearson testing with $k_i \geq 0 (i = 1, ..., M)$.

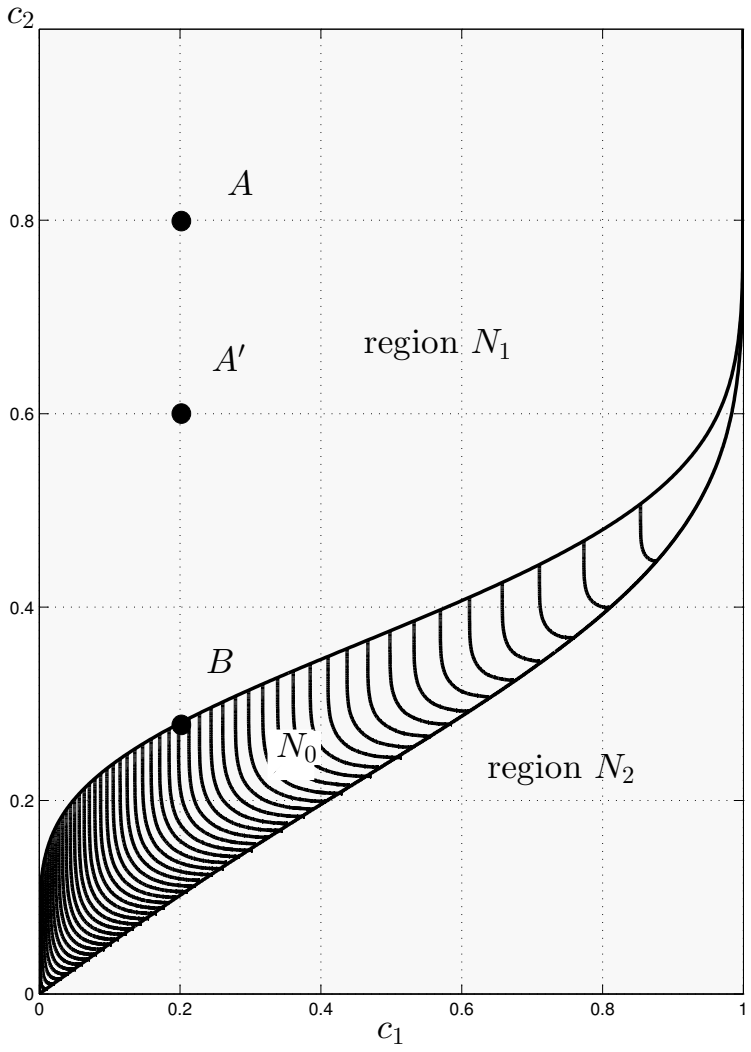

Fig. 2. Region that can be achieved by Neyman Pearson testing with $k_i \geq 0 (i = 1, ..., M)$.

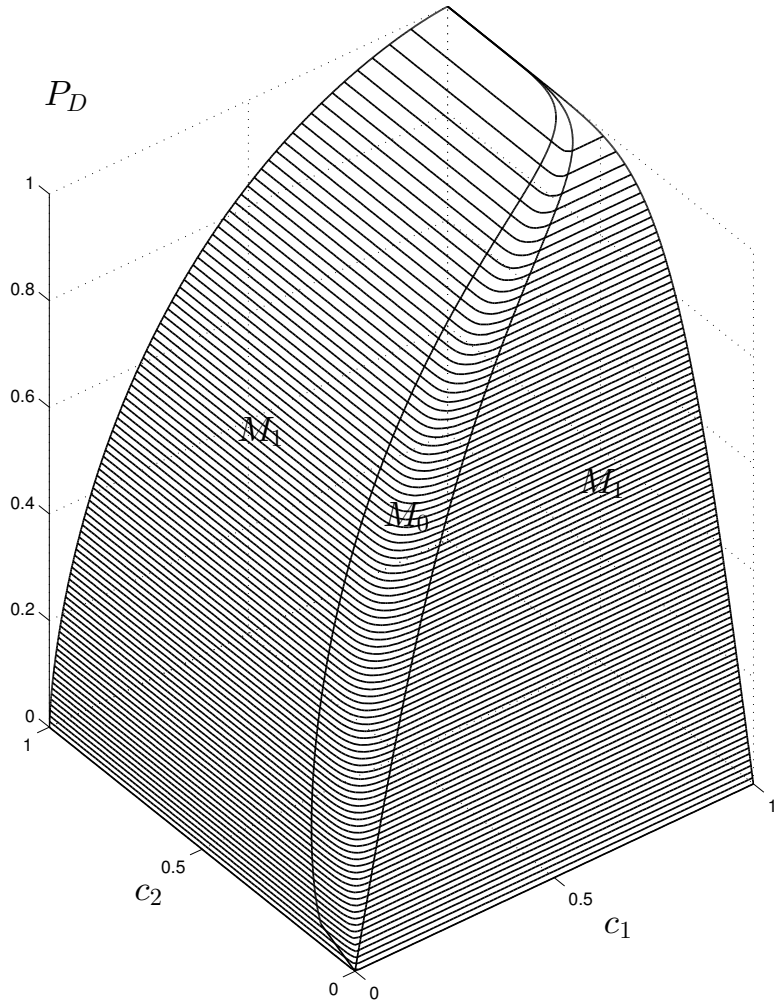

Fig. 3. The M-ROC surface for Gaussian Hypotheses.

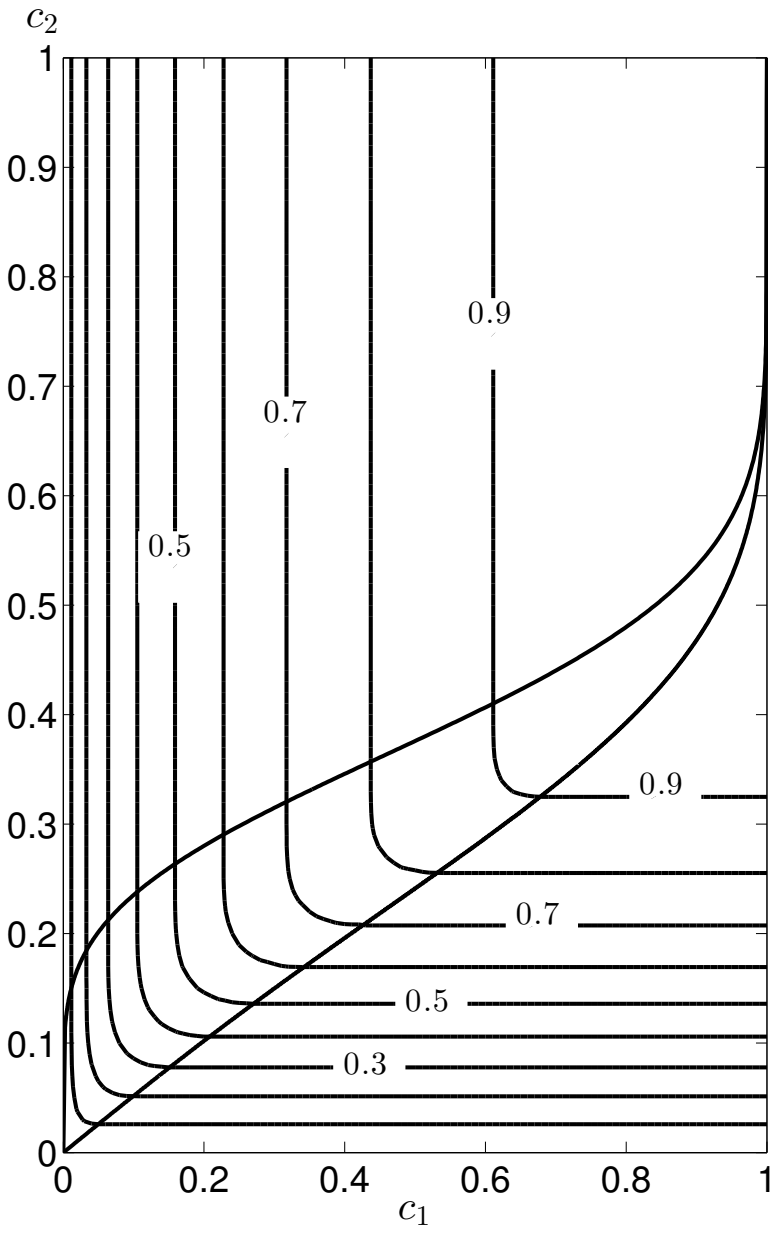

Fig. 4. Contour for M-ROC surface.

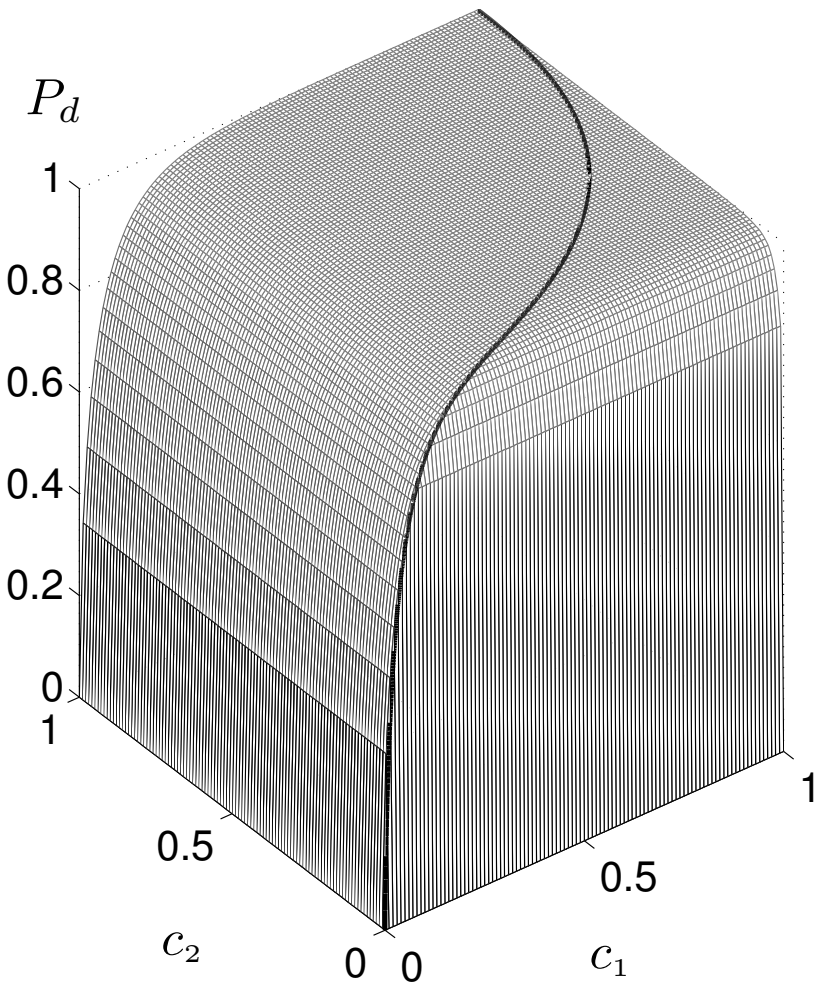

Fig. 5. The M-ROC for the Chi-square example.

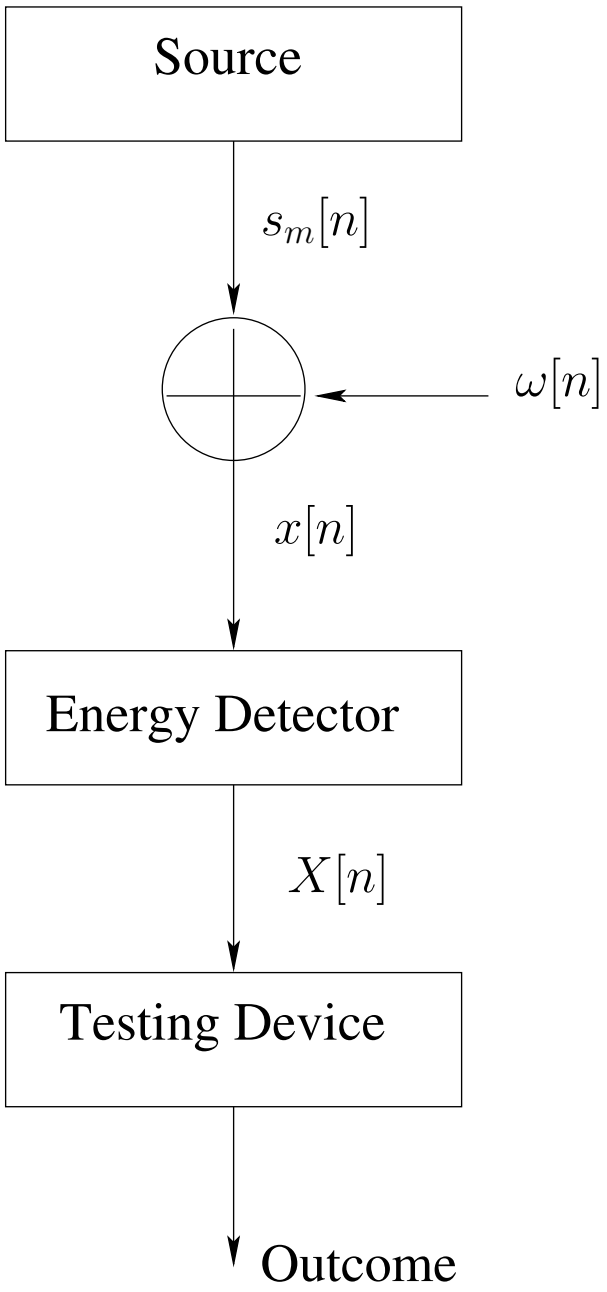

Fig. 6. The Block Diagram for Energy Based Spectrum Sensing.

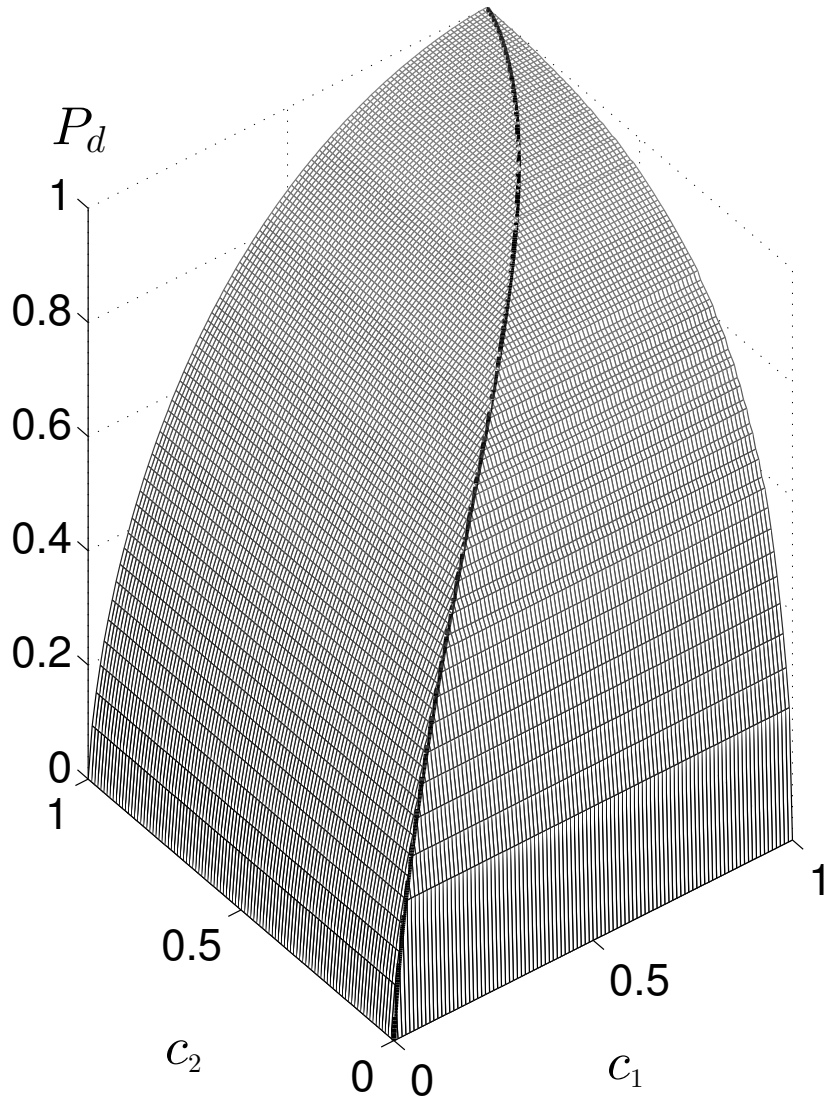

Fig. 7. Analysis performance of MENP test for $\sigma_\omega^2 = 1$, $\sigma_{s_1}^2 = 0.1$ $\sigma_{s_2}^2 = 0.15$, $N = 120$.

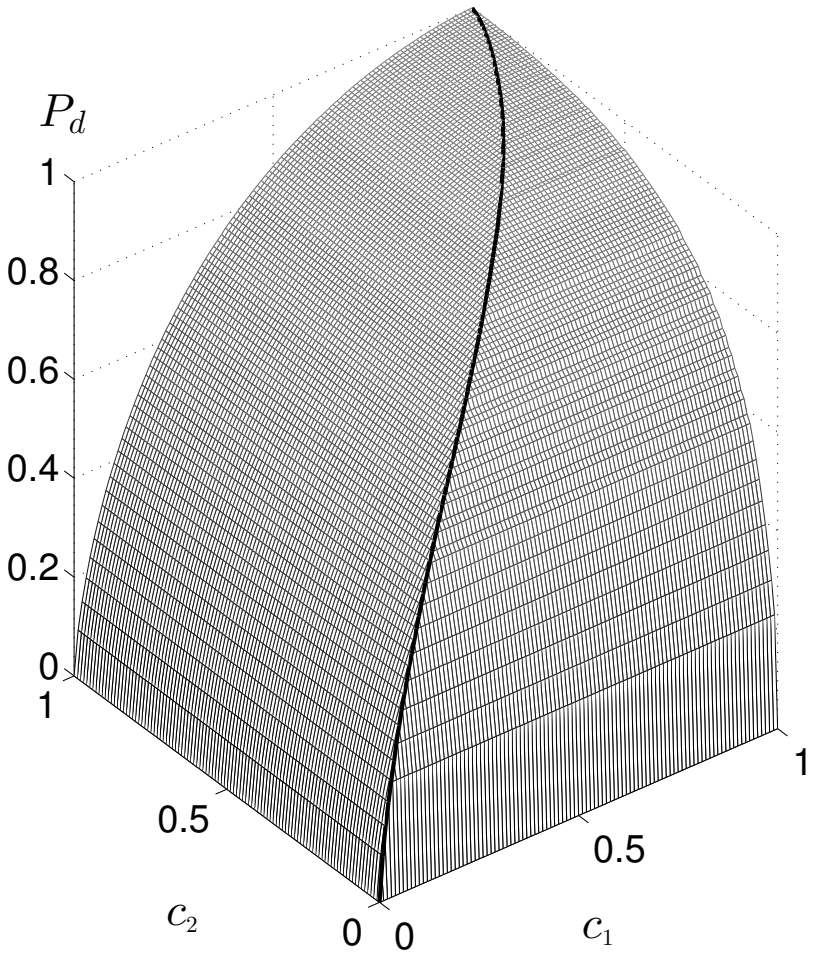

Fig. 8. Monte Carlo Simulation of MENP test for $\sigma_\omega^2 = 1$, $\sigma_{s_1}^2 = 0.1$ $\sigma_{s_2}^2 = 0.15$, $N = 120$.